Available online at http://jprm.sms.edu.pk/
Journal of Prime Research in Mathematics, 19(1) (2023), 14-26

Journal of Prime Research in Mathematics

Sombor indices of molecular graphs and some derived graphs of V-phenylenic nanotubes and nanotori

Setareh Javame[a], Massoud Ghods[b,*]

[a] Department of applied Mathematics, Semnan University, 35131-19111,Iran.
[b] Department of applied Mathematics, Semnan University, 35131-19111,Iran.

Abstract

Carbon nanotubes are widely used in various fields such as composites, energy devices, electronic applications, and medical applications. The most commonly used nanotubes and nanotubes are V-phenylenic nanotubes and nanotori. Topological analysis of a molecule involves translating its molecular structure into a unique number.
In this article, Sombor indices for molecular graph, line graph, and subdivision graph of the V-phenylenic nanotubes and nanotori are calculated.

Keywords: Topological index, molecular graph, nanotube, nanotori, line graph, subdivision graph.
2010 MSC: 05C20.

1. Introduction and Preliminaries

Carbon nanotubes (CNTs) were first discovered in 1991[13]. So far, much research has been done on their structure and the determination of their physical and chemical properties by direct measurement and prediction methods using modeling techniques. Because of the remarkable physical and chemical properties of carbon nanotubes, many scientists and industries are now working on them.
The production of carbon nanotubes is increasing exponentially every year, and as a result, their prices are decreasing. Carbon nanotubes consist of molecules with a diameter of nanometers. Also, the ratio of length to diameter is large.
One of the essential applications of nanotubes is in electronic devices [3].
Another essential feature is using nanotubes as a high-capacity hydrogen storage medium [16].
The high yang modulus and tensile strength of nanotubes have led to speculation about their possible use

*Corresponding author
Email addresses: setareh.javame@semnan.ac.ir (Setareh Javame), mghods@semnan.ac.ir (Massoud Ghods)

Received : 17 October 2022; *Accepted:* 07 February 2023; *Published Online:* 08 June 2023.

in widely used materials such as composite materials with improved mechanical properties [7, 15].
The geometric properties of nanotubes as a new tool in drug delivery have shown significant application [5]. Another essential application is their suitability as electron field emitters. A considerable advantage of SWNT materials is their use as electrochemical lithium battery electrodes with irreversible capacities and high voltage hysteresis.
For new applications of carbon nanotubes, control Diameter, chirality, number of layers, and purity are of particular importance.
Despite all efforts, the lack of reliable production capacity in high volume and the high price of nanotubes have prevented the commercialization of carbon nanotube technologies.
One of the most widely used nanotubes are the V-phenylenic nanotubes and nanotori, which have attracted the attention of many scientists in recent years due to their wide applications in the production of gas-sensitive, catalytic, and corrosion-resistant materials [14].
Figure (1) shows the molecular graph structure of the V-phenylenic nanotube. Nanotori particles have been

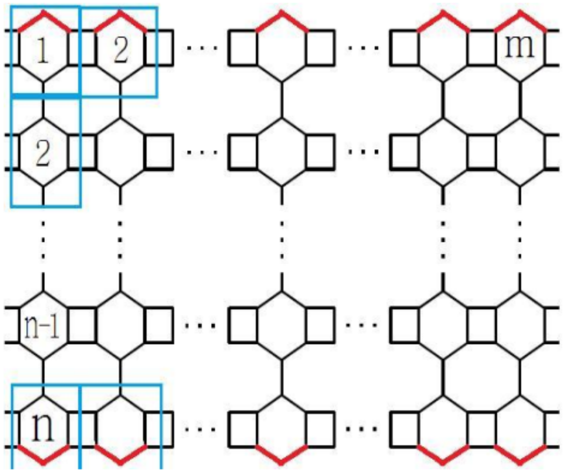

Figure 1: The molecular graph structure of V-phenylenic nanotube $VPHX[p, q]$

very promising in nanophotonic applications.
If m is the number of atoms in rows, and n is the number of atoms in columns, we show V-phenylenic and nanotransformer nanotubes as $VPHX[p, q]$, and $VPHY[p, q]$.
Figure (2) shows the molecular graph structure of the V-phenylenic nanotori.

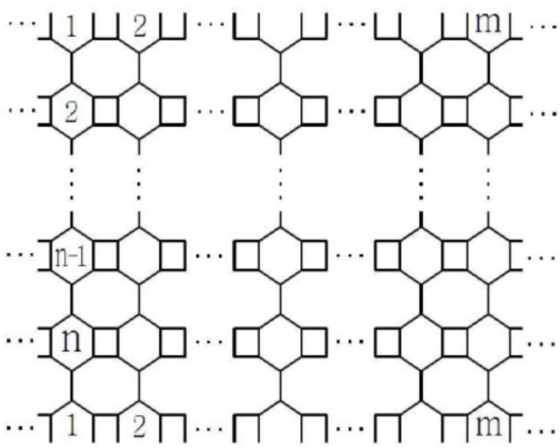

Figure 2: The molecular graph structure of V-phenylenic nanotori $VPHY[p, q]$

In [1], Pi polynomials and topological indices related to V-phenylenic nanotubes and nanotubes are calculated. In [10], Pi polynomials and some topological indices related to V-phenylenic and nanotube nanotubes are calculated. So far, many well-known topological indicators of these materials have been calculated. The Pi vertex index in [4], the Geometric-arithmetic index and atom-bond connectivity index in [11], the eccentricity connectivity index in [17], the GA_5 index in [8], the fourth atom-bond connectivity index in [9] ,and M-polynomials of V- phenylenic nanotubes and nanotori and general version of Randić index and inverse Randić index and second modified Zagreb index and Symmetric division index and harmonic index and Inverse sum-index and augmented Zagreb index in [14].
Mathematical chemistry is a branch of theoretical chemistry that discusses molecular structure using mathematical methods without considering their quantum mechanics.
The essential role of molecular descriptors is in mathematical chemistry. Chemical graph theory is a branch of mathematical chemistry that deals with the relationship between mathematics, chemistry, and graph theory.
In a molecular graph, its vertices correspond to atoms, and its edges correspond to bonds.
Topological indices are numerical values related to a chemical structure that describes the correlation of chemical structure with different physical properties and chemical reactions.

Definition 1.1. In a non-empty graph G, if each edge is considered as a vertex and the two vertices are connected, if the corresponding edges of the two vertices are adjacent to G, the resulting graph is denoted by $L(G)$ and is called the line graph of G [6].

Definition 1.2. The Subdivision graph of graph G is a graph obtained by placing an extra vertex on each edge of G. The subdivision graph is denoted by $S(G)$ [6].

The Sombor index was introduced by Gutman in late 2020 [12], and since then, many researchers have studied and researched it. We refer to [2, 18]. They have obtained numerous relationships based on it. The Sombor index for graph G is defined as:

$$SO(G) = \sum_{uv\in E(G)} \sqrt{d_u^2 + d_v^2}.$$

We also have for the reduced Sombor index and the average Sombor index, respectively:

$$\begin{aligned} SO_{red}(G) &= \textstyle\sum_{uv\in E(G)} \sqrt{(d_u-1)^2+(d_v-1)^2}, \\ SO_{avr}(G) &= \textstyle\sum_{uv\in E(G)} \sqrt{(d_u-\bar{d})^2+(d_v-\bar{d})^2}\,, \end{aligned}$$

where $\bar{d} = \frac{2|E(G)|}{|V(G)|}$.

In this article, first, we consider the molecular graphs of V-phenylenic nanotubes and V-nanotori, and calculate the respective Sombor indices. In the following, we draw the line graph and the subdivision graph of these structures, and we do the same calculations. Finally, we compare the behavior of these numerical quantities.

2. Main results

There are two types of edges in the V-phenylenic nanotubes as follows:

$$\begin{aligned} &E_1 = \{(d_u, d_v)\,|uv \in E(G), d_u = 2, d_v = 3\}\,, \\ &E_2 = \{(d_u, d_v)\,|uv \in E(G), d_u = 3, d_v = 3\}\,, \\ &|E| = |E_1| + |E_2| = 4m + 9mn - 5m = 9mn - m. \end{aligned}$$

$$\bar{d}(G) = \frac{2\,|E(G)|}{|V(G)|} = \frac{2(9mn-m)}{6mn} = \frac{9mn-m}{3mn} = \frac{9n-1}{3n}.$$

Edge type	Number of edges
E_1	4m
E_2	9mn-5m

Table 1: Types and the numbers of edges in the molecular graph of the V-phenylenic nanotubes.

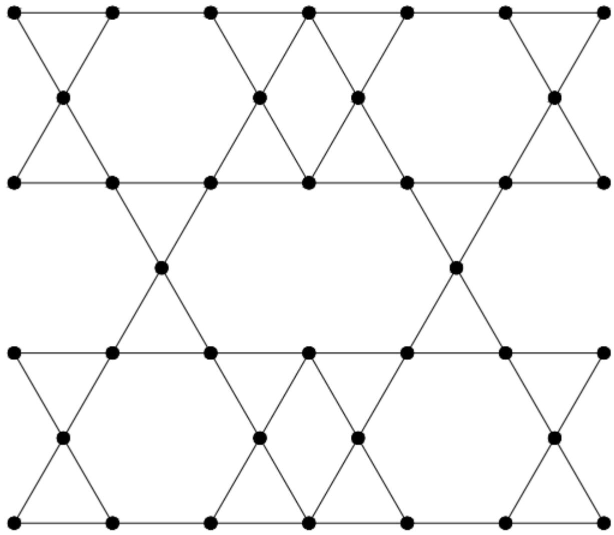

Figure 3: $L(G)$ in V-phenylenic nanotube $VPHX[p,q]$.

Figure (3) shows the line graph of the V-phenylenic nanotube.
There are three types of edges in the line graph of the V-phenylenic nanotubes as follows:

$$E_1 = \{(d_u, d_v)\,|uv \in E(L(G)), d_u = 3, d_v = 3\},$$
$$E_2 = \{(d_u, d_v)\,|uv \in E(L(G)), d_u = 3, d_v = 4\}, \qquad E_3 = \{(d_u, d_v)\,|uv \in E(L(G)), d_u = 4, d_v = 4\}.$$

Edge type	Number of edges
E_1	2m
E_2	8m
E_3	18mn-14m

Table 2: Types and the numbers on edges for $L(G)$ in V-phenylenic nanotubes.

As a result, the number of edges and vertices in the line graph of the V-phenylenic nanotube is equal to:

$$|E(L(G))| = 18mn - 4m,$$
$$|V(L(G))| = |E(G)| = 9mn - m.$$

We have,

$$\bar{d}(L(G)) = \frac{2\,|E(L(G))|}{|V(L(G))|} = \frac{2(18mn - 4m)}{9mn - m} = \frac{36n - 8}{9n - 1}.$$

Figure (4) shows the subdivision graph of the V-phenylenic nanotube.
There are two types of edges in subdivision graph of V-phenylenic nanotube as follows:

$$E_1 = \{(d_u, d_v)\,|uv \in E(S(G)), d_u = 2, d_v = 2\},$$
$$E_2 = \{(d_u, d_v)\,|uv \in E(S(G)), d_u = 2, d_v = 3\}.$$

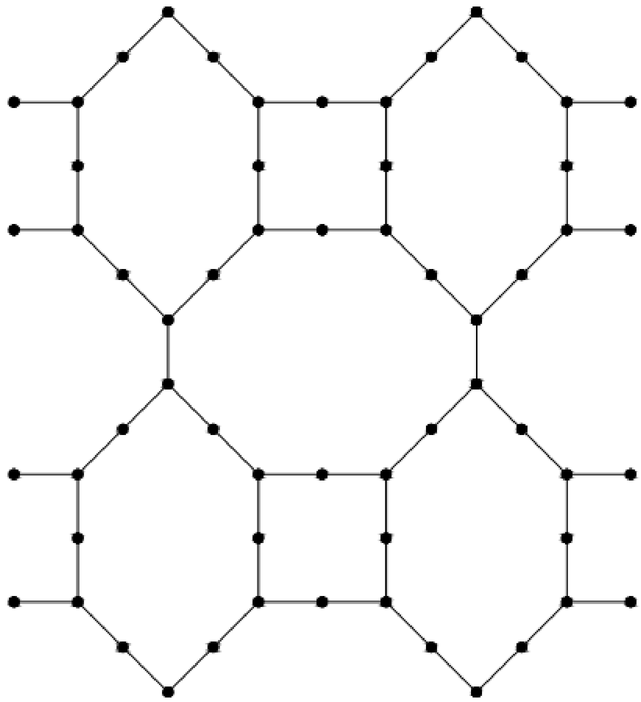

Figure 4: $S(G)$ for V-phenylenic nanotube $VPHX[p,q]$.

Edge type	Number of edges
E_1	4m
E_2	18mn-6m

Table 3: Types and the numbers on edges for $S(G)$ in V-phenylenic nanotube.

As a result, the number of edges and vertices in the subdivision graph of the V-phenylenic nanotube is equal to:

$$|E(S(G))| = |E_1| + |E_2| = 4m + 18mn - 6m = 18mn - 2m,$$
$$|V(S(G))| = |E(G)| + |V(G)| = 15mn - m.$$

We have,

$$\bar{d}(S(G)) = \frac{2\,|E(S(G))|}{|V(S(G))|} = \frac{2(18mn - 2m)}{15mn - m} = \frac{36mn - 4m}{15mn - m} = \frac{36n - 4}{15n - 1}.$$

Theorem 2.1. *Let G be the graph of the V-phenylenic nanotube. Then,*

$i)SO(G) = 9\sqrt{18}mn + (4\sqrt{13} - 5\sqrt{18})m,$

$ii)SO_{red}(G) = 9\sqrt{8}mn + (4\sqrt{5} - 5\sqrt{8})m,$

$iii)SO_{avr}(G) = \frac{9\sqrt{2}}{3n}mn + 4[\sqrt{2(\frac{9n-1}{3n})^2 - 10(\frac{9n-1}{3n}) + 13} - \frac{5\sqrt{2}}{3n}]m.$

Proof.

$$i)SO(G) = \sum_{uv \in E(G)} \sqrt{d_u^2 + d_v^2} = \sum_{uv \in E_1(G)} \sqrt{d_u^2 + d_v^2} + \sum_{uv \in E_2(G)} \sqrt{d_u^2 + d_v^2}$$
$$= 4m(\sqrt{13}) + (9mn - 5m)(\sqrt{18}) = 9\sqrt{18}mn + (4\sqrt{13} - 5\sqrt{18})m,$$

$$
\begin{aligned}
ii) SO_{red}(G) &= \sum_{uv \in E(G)} \sqrt{(d_u-1)^2+(d_v-1)^2} \\
&= \sum_{uv \in E_1(G)} \sqrt{(d_u-1)^2+(d_v-1)^2} + \sum_{uv \in E_2(G)} \sqrt{(d_u-1)^2+(d_v-1)^2} \\
&= 4m(\sqrt{5}) + (9mn-5m)(\sqrt{8}) = 9\sqrt{8}mn + (4\sqrt{5}-5\sqrt{8})m,
\end{aligned}
$$

$$
\begin{aligned}
iii) SO_{avr}(G) &= \sum_{uv \in E(G)} \sqrt{(d_u-\bar{d})^2+(d_v-\bar{d})^2} \\
&= \sum_{uv \in E_1(G)} \sqrt{(d_u-\bar{d})^2+(d_v-\bar{d})^2} + \sum_{uv \in E_2(G)} \sqrt{(d_u-\bar{d})^2+(d_v-\bar{d})^2} \\
&= 4m(\sqrt{(2-\frac{9n-1}{3n})^2+(3-\frac{9n-1}{3n})^2}) + (9mn-5m)(\sqrt{(3-\frac{9n-1}{3n})^2+(3-\frac{9n-1}{3n})^2}) \\
&= 4m(\sqrt{2(\frac{9n-1}{3n})^2-10(\frac{9n-1}{3n})+13}) + (9mn-5m)(\sqrt{2}\left|3-\frac{9n-1}{3n}\right|) \\
&= \frac{9\sqrt{2}}{3n}mn + 4[\sqrt{2(\frac{9n-1}{3n})^2-10(\frac{9n-1}{3n})+13} - \frac{5\sqrt{2}}{3n}]m.
\end{aligned}
$$

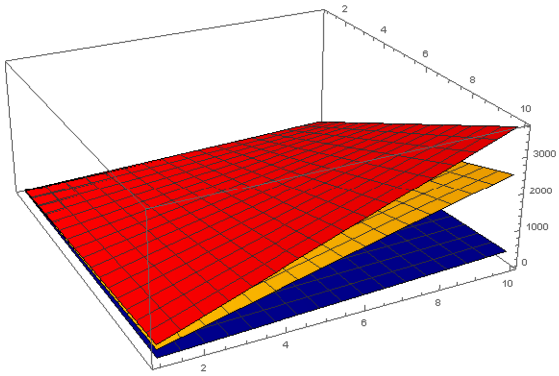

Figure 5: Shows the behavior of the $SO(G), SO_{red}(G)$, and the $SO_{avr}(G)$, with Red, Yellow, and Blue, respectively, in the molecular graph of the V-phenylenic nanotube.

□

Theorem 2.2. *Let $L(G)$ be the line graph of V-phenylenic nanotube. Then,*

$i) SO(L(G)) = 18\sqrt{32}mn + (2\sqrt{18} - 14\sqrt{32} + 40)m,$

$ii) SO_{red}(L(G)) = 18\sqrt{18}mn + (2\sqrt{8} + 8\sqrt{13} - 14\sqrt{18})m,$

$iii) SO_{avr}(L(G)) = (\sqrt{2}\left|\frac{4}{9n-1}\right|)mn + [2(\sqrt{2}\left|\frac{-9n+5}{9n-1}\right|) + 8\sqrt{2(\frac{36n-8}{9n-1})^2 - 14(\frac{36n-8}{9n-1}) + 25} - \frac{54\sqrt{2}}{9n-1}]m.$

Proof.

$$
\begin{aligned}
i) SO(L(G)) &= \sum_{uv \in E(L(G))} \sqrt{d_u^2+d_v^2} = \sum_{uv \in E_1(L(G))} \sqrt{d_u^2+d_v^2} + \sum_{uv \in E_2(L(G))} \sqrt{d_u^2+d_v^2} + \sum_{uv \in E_3(L(G))} \sqrt{d_u^2+d_v^2} \\
&= 2m(\sqrt{18}) + 8m(5) + (18mn-14m)(\sqrt{32}) = 2\sqrt{18}m + 40m + (18mn-14m)(\sqrt{32}) \\
&= 18\sqrt{32}mn + (2\sqrt{18} - 14\sqrt{32} + 40)m,
\end{aligned}
$$

$$
\begin{aligned}
ii)SO_{red}(L(G)) &= \sum_{uv\in E(L(G))} \sqrt{(d_u-1)^2+(d_v-1)^2} \\
&= \sum_{uv\in E_1(L(G))} \sqrt{(d_u-1)^2+(d_v-1)^2} + \sum_{uv\in E_2(L(G))} \sqrt{(d_u-1)^2+(d_v-1)^2} \\
&\quad + \sum_{uv\in E_3(L(G))} \sqrt{(d_u-1)^2+(d_v-1)^2} \\
&= 2m(\sqrt{8}) + 8m(\sqrt{13}) + (18mn-14m)(\sqrt{18}) = 2\sqrt{8}m + 8\sqrt{13}m + (18mn-14m)(\sqrt{18}) \\
&= 18\sqrt{18}mn + (2\sqrt{8}+8\sqrt{13}-14\sqrt{18})m,
\end{aligned}
$$

$$
\begin{aligned}
iii)SO_{avr}(L(G)) &= \sum_{uv\in E(L(G))} \sqrt{(d_u-\bar{d})^2+(d_v-\bar{d})^2} \\
&= \sum_{uv\in E_1(L(G))} \sqrt{(d_u-\bar{d})^2+(d_v-\bar{d})^2} + \sum_{uv\in E_2(L(G))} \sqrt{(d_u-\bar{d})^2+(d_v-\bar{d})^2} \\
&\quad + \sum_{uv\in E_3(L(G))} \sqrt{(d_u-\bar{d})^2+(d_v-\bar{d})^2} \\
&= 2m\left(\sqrt{(3-\frac{36n-8}{9n-1})^2+(3-\frac{36n-8}{9n-1})^2}\right) + 8m\left(\sqrt{(3-\frac{36n-8}{9n-1})^2+(4-\frac{36n-8}{9n-1})^2}\right) \\
&\quad + (18mn-14m)\left(\sqrt{(4-\frac{36n-8}{9n-1})^2+(4-\frac{36n-8}{9n-1})^2}\right) \\
&= 2m\left(\sqrt{2}\left|3-\frac{36n-8}{9n-1}\right|\right) + 8m\left(\sqrt{2(\frac{36n-8}{9n-1})^2-14(\frac{36n-8}{9n-1})+25}\right) \\
&\quad + (18mn-14m)\left(\sqrt{2}\left|4-\frac{36n-8}{9n-1}\right|\right) \\
&= \left(\sqrt{2}\left|\frac{4}{9n-1}\right|\right)mn + \left[2\left(\sqrt{2}\left|\frac{-9n+5}{9n-1}\right|\right) + 8\sqrt{2(\frac{36n-8}{9n-1})^2-14(\frac{36n-8}{9n-1})+25} - \frac{54\sqrt{2}}{9n-1}\right]m.
\end{aligned}
$$

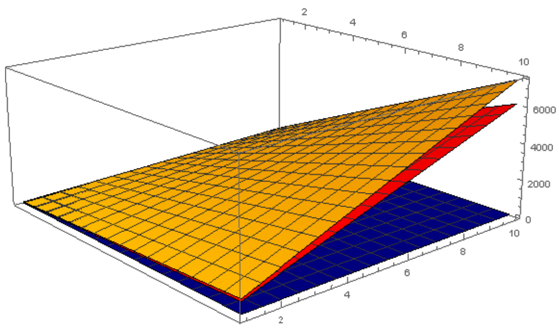

Figure 6: Shows the behavior of the $SO(L(G)), SO_{red}(L(G))$, and the $SO_{avr}(L(G))$, with Red, Yellow, and Blue, respectively, for the V-phenylenic nanotube.

$\square$

Theorem 2.3. *Let $S(G)$ be the subdivision graph of the V-phenylenic nanotube. Then,*

$i)SO(S(G)) = 18\sqrt{13}mn + (4\sqrt{8}-6\sqrt{13})m,$

$ii)SO_{red}(S(G)) = 18\sqrt{5}mn + (4\sqrt{2}-6\sqrt{5})m,$

$iii)SO_{avr}(S(G)) = [4\sqrt{2}\left|\frac{-6n+2}{15n-1}\right| - 6(\sqrt{13+10(\frac{36n-4}{15n-1})+2(\frac{36n-4}{15n-1})^2})]m + 18(\sqrt{13+10(\frac{36n-4}{15n-1})+2(\frac{36n-4}{15n-1}$

Proof.

$$i) SO(S(G)) = \sum_{uv\in E_1(S(G))} \sqrt{d_u^2+d_v^2} + \sum_{uv\in E_2(S(G))} \sqrt{d_u^2+d_v^2} = 4\sqrt{8}m + (18mn-6m)\sqrt{13}$$
$$= 18\sqrt{13}mn + (4\sqrt{8}-6\sqrt{13})m,$$

$$ii) SO_{red}(S(G)) = \sum_{uv\in E_1(S(G))} \sqrt{(d_u-1)^2+(d_v-1)^2} + \sum_{uv\in E_2(S(G))} \sqrt{(d_u-1)^2+(d_v-1)^2}$$
$$= 4\sqrt{2}m + (18mn-6m)\sqrt{5} = 18\sqrt{5}mn + (4\sqrt{2}-6\sqrt{5})m,$$

$$iii) SO_{avr}(S(G)) = \sum_{uv\in E_1(S(G))} \sqrt{(d_u-\bar{d})^2+(d_v-\bar{d})^2} + \sum_{uv\in E_2(S(G))} \sqrt{(d_u-\bar{d})^2+(d_v-\bar{d})^2}$$
$$= 4m(\sqrt{2(2-\frac{36n-4}{15n-1})^2} + (18mn-6m)\sqrt{(2-\frac{36n-4}{15n-1})^2+(3-\frac{36n-4}{15n-1})^2}$$
$$= 4m(\sqrt{2}\left|\frac{-6n+2}{15n-1}\right|) + (18mn-6m)(\sqrt{13+10(\frac{36n-4}{15n-1})+2(\frac{36n-4}{15n-1})^2})$$
$$= [4\sqrt{2}\left|\frac{-6n+2}{15n-1}\right| - 6(\sqrt{13+10(\frac{36n-4}{15n-1})+2(\frac{36n-4}{15n-1})^2})]m$$
$$+ 18(\sqrt{13+10(\frac{36n-4}{15n-1})+2(\frac{36n-4}{15n-1})^2})mn.$$

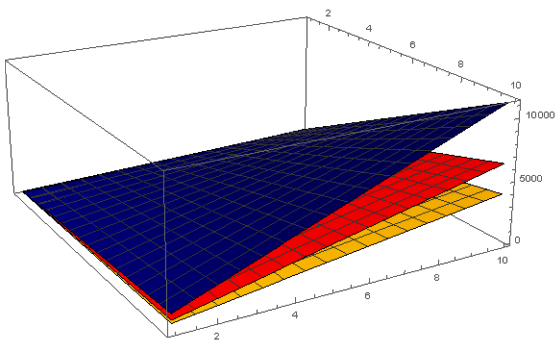

Figure 7: Shows the behavior of the $SO(S(G)), SO_{red}(S(G))$, and the $SO_{avr}(S(G))$, with Red, Yellow, and Blue, respectively, for the V-phenylenic nanotube.

□

There is one type of edge in the V-phenylenic nanotori as follows:

$$E_1 = \{(d_u, d_v)\,|uv \in E(H), d_u = 3, d_v = 3\}.$$

$$\bar{d}(H) = \frac{2\,|E(H)|}{|V(H)|} = \frac{2(9mn)}{6mn} = \frac{18mn}{6mn} = 3.$$

Edge type	Number of edges
E_1	9mn

Table 4: Types and the numbers of edges in the molecular graph structure of the V-phenylenic nanotori.

Figure (8) shows the line graph of the V-phenylenic nanotori.

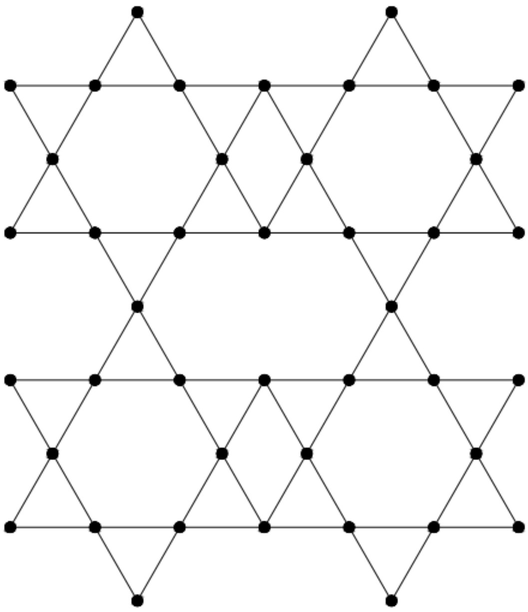

Figure 8: $L(G)$ for V-phenylenic nanotori.

Edge type	Number of edges
E_1	18mn

Table 5: Types and the numbers of edges for $L(G)$ in V-phenylenic nanotori.

There is one type of edge in the line graph of the V-phenylenic nanotori as follows:

$$E_1 = \{(d_u, d_v)\,|uv \in E(L(H)), d_u = 4, d_v = 4\}.$$

As a result, the number of edges and vertices in the line graph of the V-phenylenic nanotori is equal to:

$$|E(L(H))| = 18mn,$$
$$|V(L(H))| = |E(H)| = 9mn.$$

We have,

$$\bar{d}(L(H)) = \frac{2\,|E(H)|}{|V(H)|} = \frac{2(18mn)}{9mn} = \frac{36mn}{9mn} = 4.$$

Figure (9) shows the subdivision graph of the V-phenylenic nanotori.
There is one type of edge in the subdivision graph of the V-phenylenic nanotori as follows:

$$E_1 = \{(d_u, d_v)\,|uv \in E(S(H)), d_u = 2, d_v = 3\}.$$

Edge type	Number of edges
E_1	18mn

Table 6: Types and the numbers of edges for $S(G)$ in V-phenylenic nanotori.

As a result, the number of edges and vertices in the subdivision graph of the V-phenylenic nanotori is equal to:

$$|E(S(H))| = 18mn,$$
$$|V(S(H))| = |E(H)| + |V(H)| = 15mn.$$

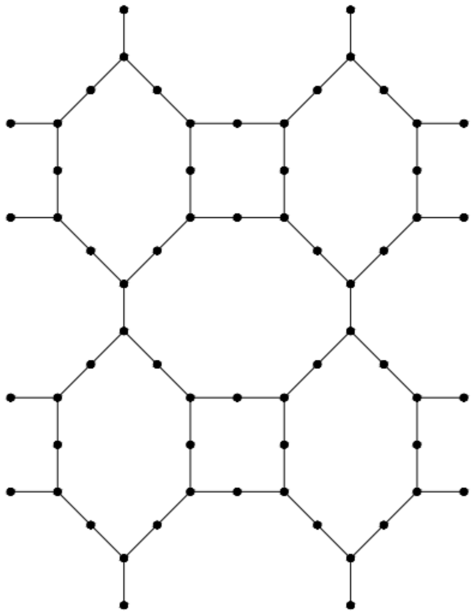

Figure 9: $S(G)$ for V-phenylenic nanotori.

We have,

$$\bar{d}(G) = \frac{2\,|E(S(H))|}{|V(S(H))|} = \frac{2(18mn)}{15mn} = \frac{36mn}{15mn} = \frac{12}{5}.$$

Theorem 2.4. *Let H be the graph of the V-phenylenic nanotori. Then,*

$i)SO(H) = 9\sqrt{18}mn,$
$ii)SO_{red}(H) = 9\sqrt{8}mn,$
$iii)SO_{avr}(H) = 0.$

Proof.

$$i)SO(H) = \sum_{uv\in E_1(H)} \sqrt{d_u^2 + d_v^2} = 9\sqrt{18}mn,$$

$$ii)SO_{red}(H) = \sum_{uv\in E_1(H)} \sqrt{(d_u-1)^2 + (d_v-1)^2} = 9\sqrt{8}mn,$$

$$iii)SO_{avr}(H) = \sum_{uv\in E_1(H)} \sqrt{(d_u-\bar{d})^2 + (d_v-\bar{d})^2} = 9mn \times 0 = 0.$$

□

Theorem 2.5. *Let $L(H)$ be the line graph of the V-phenylenic nanotori. Then,*

$i)SO(L(H)) = 72\sqrt{2}mn,$
$ii)SO_{red}(L(H)) = 54\sqrt{2}mn,$
$iii)SO_{avr}(L(H)) = 0.$

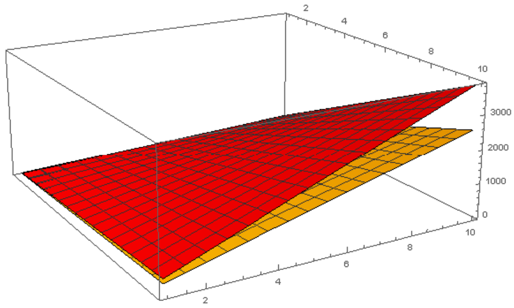

Figure 10: Shows the behavior of the $SO(G), SO_{red}(G)$, and the $SO_{avr}(G)$, with Red, Yellow, and Blue, respectively, for the molecular graph of the V-phenylenic nanotori.

Proof.

$$i) SO(L(H)) = \sum_{uv \in E_1(H)} \sqrt{d_u^2 + d_v^2} = 18\sqrt{32}mn = 72\sqrt{2}mn,$$

$$ii) SO_{red}(L(H)) = \sum_{uv \in E_1(H)} \sqrt{(d_u - 1)^2 + (d_v - 1)^2} = 18\sqrt{18}mn = 54\sqrt{2}mn,$$

$$iii) SO_{avr}(L(H)) = \sum_{uv \in E_1(H)} \sqrt{(d_u - \bar{d})^2 + (d_v - \bar{d})^2} = 18mn(0) = 0.$$

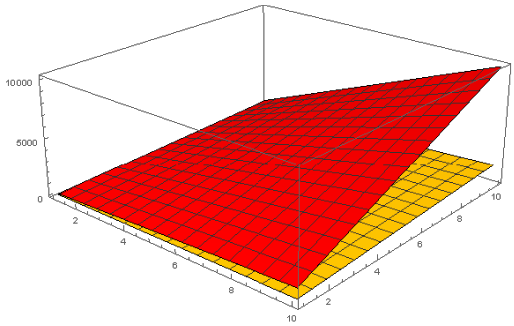

Figure 11: Shows the behavior of the $SO(L(G)), SO_{red}(L(G))$, and the $SO_{avr}(L(G))$, with Red, Yellow, and Blue, respectively, for the V-phenylenic nanotori

□

Theorem 2.6. *Let $S(H)$ be the subdivision graph of the V-phenylenic nanotori. Then,*

$i) SO(S(H)) = 18\sqrt{13}mn,$

$ii) SO_{red}(S(H)) = 18\sqrt{5}mn,$

$iii) SO_{avr}(S(H)) = \dfrac{18\sqrt{13}}{5}mn.$

Proof.

$$i) SO(S(H)) = \sum_{uv \in E_1(H)} \sqrt{d_u^2 + d_v^2} = 18\sqrt{13}mn,$$

$$ii) SO_{red}(S(H)) = \sum_{uv \in E_1(H)} \sqrt{(d_u - 1)^2 + (d_v - 1)^2} = 18\sqrt{5}mn,$$

$$iii) SO_{avr}(S(H)) = \sum_{uv \in E_1(H)} \sqrt{(d_u - \bar{d})^2 + (d_v - \bar{d})^2} = 18mn(\sqrt{(2 - \frac{12}{5})^2 + (3 - \frac{12}{5})^2}) = \frac{18\sqrt{13}}{5}mn.$$

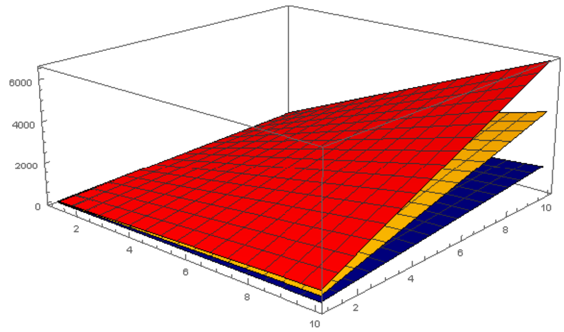

Figure 12: Shows the behavior of the $SO(S(G)), SO_{red}(S(G))$, and the $SO_{avr}(S(G))$, with Red, Yellow, and Blue, respectively, for the V-phenylenic. nanotori.

□

Acknowledgements:

This research did not receive any specific grant from funding agencies in the public, commercial, or not-for-profit sectors.

3. Conclusion

In this article, Sombor indices were calculated for V-phenylenic nanotubes and nanotori and their line graph and subdivision graph. In nanotori, the Sombor index always has the highest value compared to the reduced Sombor index and the average Sombor index in the molecular graph, line graph, and subdivision graph.

In the nanotube, the average Sombor index has the lowest value compared to the Sombor index and the reduced Sombor index in the molecular graph and the line graph, still, in the subdivision graph, the average Sombor index has the highest value.

References

[1] V. Alamian, A. Bahrami and B. Edalatzadeh, *PI Polynomial of V-phenylenic nanotubes and nanotori*, Int. J. Mol. Sci. **9:3** (2008), 229–234. 1

[2] A. Alsinai, B. Basavanagoud, M. Sayyed and M. R. Farahani, *Sombor index of some nanostructures*, J. Prime Res. Math. **17:2** (2021), 123–133. 1

[3] Ph. Avouris, *Carbon nanotubes: nanomechanics, manipulation, and electronic devices*, Appl. Surf. Sci. **141:3** (1999), 201-209. 1

[4] A. Bahrami and J. Yazdani, *Vertex PI index of V-phenylenic nanotubes and nanotori*, Dig. J. Nanomater. Biostructures. **4:1** (2009), 141–144. 1

[5] M. S. Dresselhaus, G. Dresselhaus and P. C. Eklund, *Science of fullerenes and carbon nanotubes*, Academic Press, San Diego, (1996). 1

[6] M. Eliasi and B. Taeri, *Four new sums of graphs and their wiener indices*, Discret. Appl. Math. **157** (2009), 794–803. 1.1, 1.2

[7] M. Endo, T. Hayashi, Y. A. Kim and H. Muramatsu, *Development and application of carbon nanotubes*, Jpn. J. Appl. Phys. **45:6R** (2006), 4883. 1

[8] M. R. Farahani, *Computing GA_5 index of V-phenylenic nanotubes and nanotori*, Int. J. Chem Model. **5:4** (2013), 479–484. 1

[9] M. R. Farahani, *Computing fourth atom-bond connectivity index of V-phenylenic nanotubes and nanotori*, Acta Chim. Slov. **60:2** (2013), 429–432. 1

[10] M. R. Farahani, *Computing theta polynomial, and theta index of V-phenylenic planar, nanotubes and nanotoris*, Int. J. Theoretical Chemistry, **1:1** (2013), 01–09. 1

[11] M. Ghorbani, H. Mesgarani and S. Shakeraneh, *Computing GA index and ABC index of -phenylenic nanotube*, Optoelectron. Adv. Mater.-Rapid Commun. **5:3** (2011), 324–326. 1

[12] A. Gutman, I, *Geometric approach to degree-based topological indices: Sombor indices*, MATCH Commun. Math. Comput. Chem. **86:1** (2021), 11-16. 1
[13] S. Iijima, *Helical microtubules of graphitic carbon*, Nature. **354**, (1991), 56-58. 1
[14] Y.C. Kwun, M. Munir, W. Nazeer, S. Rafique and S. Min Kang, *M-Polynomials and topological indices of V-phenylenic Nanotubes and Nanotori*, Scientific reports. **7:1** (2017), 1-9. 1, 1
[15] G. Overney, W. Zhong and D. Tománek, *Structural rigidity and low frequency vibrational modes of long carbon tubules*, Z. Phys. **27** (1993), 93–96.
[16] V. N. Popov, *Carbon nanotubes: properties and application*, Mater. Sci. Eng: R: Reports. **43:3** (2004), 61-102. 1 1
[17] N.P. Rao and K.L. Lakshmi, *Eccentricity connectivity index of V-phenylenic nanotubes*, Dig. J. Nanomater. Biostructures. **6:1** (2010), 81–87. 1
[18] N.K. Raut, and G.K. Sanap, *On Sombor indices of $VC_5C_7[p,q]$ nanotubes by M-polynomial and exponential*, Journal of Research in Applied Mathematics, **8:6** (2022), 64–70. 1